

Interannual
correlations between
SST and Chl *a*

H. Herrera-Cervantes
et al.

This discussion paper is/has been under review for the journal Ocean Science (OS).
Please refer to the corresponding final paper in OS if available.

Interannual correlations between sea surface temperature and concentration of chlorophyll pigment off Punta Eugenia, Baja California during different remote forcing conditions

H. Herrera-Cervantes¹, S. E. Lluch-Cota², D. B. Lluch-Cota², and G. Gutiérrez-de-Velasco¹

¹Unidad La Paz, Centro de Investigación Científica y de Educación Superior de Ensenada (CICESE), La Paz, Baja California Sur 23050, México

²Centro de Investigaciones Biológicas del Noroeste (CIBNOR), Instituto Politécnico Nacional 195, La Paz, Baja California Sur 23096, México

Received: 26 April 2013 – Accepted: 11 May 2013 – Published: 29 May 2013

Correspondence to: H. Herrera-Cervantes (hherrera@cicese.mx)

Published by Copernicus Publications on behalf of the European Geosciences Union.

Title Page

Abstract

Introduction

Conclusions

References

Tables

Figures

⏪

⏩

◀

▶

Back

Close

Full Screen / Esc

Printer-friendly Version

Interactive Discussion

Abstract

Interannual correlation between satellite-derived sea surface temperature (SST) and surface chlorophyll *a* (Chl *a*) are examined in the coastal upwelling zone off Punta Eugenia on the west coast of the Baja California Peninsula, area identified as intense biological productivity and oceanographic transition between mid-latitude and tropical ocean conditions. We used empirical orthogonal functions (EOF) analysis separately and jointly on the two fields from 1997 through 2007, a time period dominated by different remote forcing; ENSO conditions (weak, moderate and strong) and the largest intrusion of subarctic water reported in the last 50 yr. Coastal Upwelling Index anomalies (CUI) and the Multivariate ENSO Index (MEI) were used to identify the influence of local (wind stress) and remote (ENSO) forcing over the interannual variability of both variables. The individual EOF₁ analysis showed the greater variability of SST and Chl *a* offshore, their corresponding amplitude time series presented the highest peaks during the intrusion of subarctic water (2002–2004) and were significantly correlated with the MEI ($R_{\text{SST}} \approx 0.68$, $R_{\text{Chl } a} \approx -0.30$, $P < 0.001$) and moderately correlated with the CUI ($R_{\text{SST}} \approx -0.4$, $R_{\text{Chl } a} \approx 0.25$, $P < 0.001$), showing similar trends. The joint EOF₁ and the SST–Chl *a* correlations pattern show the area where both variables covary tightly; a band near to the coast with the largest correlations ($R > |0.4|$) mainly regulated by ENSO cycles. This was revealed when we calculate the homogeneous correlations for the periods El Niño–La Niña and the intrusion of subarctic water. Both, SST and Chl *a* showed higher coupling and two distinct physical-biological responses; on average ENSO influence were clearly along the coast mostly in SST while the subarctic water influence, were observed offshore mostly in Chl *a*. We found a coastal chlorophyll bloom correlated strongly with high wind stress anomalies that reach the coast off Punta Eugenia during spring and summer 2002 and continued its presence during 2003 which showed an enrichment pattern similar to that observed at high latitudes ($\sim 40^\circ \text{N}$). This observation may provide an explanation of why Punta Eugenia is one of the most important biological action centers.

Interannual correlations between SST and Chl *a*

H. Herrera-Cervantes et al.

Title Page

Abstract

Introduction

Conclusions

References

Tables

Figures

◀

▶

◀

▶

Back

Close

Full Screen / Esc

Printer-friendly Version

Interactive Discussion



1 Introduction

Continuous oceanographic observations carried out on the west coast of Baja California by the CalCOFI (California Cooperative Oceanic Fisheries Investigations) and IMECOCAL (Mexican Research of the California Current) programs have helped define the region of Punta Eugenia (Fig. 1) as oceanographic transitional zone (Durazo and Baumgartner, 2002), where the southern part of the California Current (CC) and the North Equatorial Current (NEC) interact at a global scale. The area is also influenced by warm and dense water originating in the Gulf of California (Parés-Sierra et al., 1997), creating a complex mixing zone between coastal and oceanic flows and intense mesoscale variability characterized by a complex pattern of filaments, meanders, and semi-permanent eddy structures (Gallaudet and Simpson, 1994). These structures carry nutrient-rich coastal waters to deep areas, causing important seasonal variability and inter-annual and very long-term changes (Espinosa-Carreón et al., 2004).

Seasonal wind forcing over the Punta Eugenia area is controlled regionally by the position and intensity of the North Pacific high pressure and the California semi-permanent low thermal (Parés-Sierra et al., 1997). This wind pattern generates an intense coastal upwelling process that, together with the local contribution of the coastal lagoons (Guerrero Negro, Ojo de Liebre, and San Ignacio), produces one of the most important Biological Action Centers of the western coast of North America, which is characterized by above average pigment concentrations (Lluch-Belda et al., 2000). The coastal ecosystem of this region is a natural refuge and a feeding and breeding area for many ecological and commercially important species (gray whale, sea turtles, spiny lobster, abalone, and clams). Maintenance of this ecosystem is based on three factors: rich coastal waters associated with an intense upwelling regime, successful implementation of cooperatives to safeguard existing resources, and relative isolation. These factors help support the fishery resource in this area, where red lobster (value of 65 milliondollarsyr⁻¹; Vega, et al., 2010; SAGARPA, 2011), abalone (value

OSD

10, 853–882, 2013

Interannual correlations between SST and Chl *a*

H. Herrera-Cervantes et al.

Title Page

Abstract

Introduction

Conclusions

References

Tables

Figures

⏪

⏩

◀

▶

Back

Close

Full Screen / Esc

Printer-friendly Version

Interactive Discussion



of 26 milliondollarsyr⁻¹; SAGARPA, 2001), and extraction of salt by solar evaporation (7000 tyr⁻¹; SEMARNAT, 1997) contributes to the economy of the entire peninsula.

Oceanographic features off the west coast of the Baja California Peninsula are dramatically affected by global-scale ENSO and interdecadal variability. El Niño events have a negative effect on fisheries: an increase in SST, high sea level, change in composition of the zooplankton community, and microbial pollution (Strub and James, 2002; Lavaniegos et al., 2002; Boehm et al., 2004). Larval reproduction and embryonic development of spiny lobster (*Panulirus interruptus*) are heavily impacted because the onset and duration of larval development is accelerated or delayed, which dramatically reduces the captures in this region (Vega, 2003). Carreón-Palau et al. (2003) and Muciño-Días et al. (2004), describe overfishing of abalone because survival, growth, and larval recruitment are heavily dependent on cooler environmental conditions. These relationships between biological and environmental factors demonstrate strong physical-biological coupling in this region.

Climate effects on SST and Chl *a* in this coastal environment are documented here for more than a decade of satellite measurements (1997–2007), period defined by Behrenfeld et al. (2006) as a permanent El Niño conditions that include the different ENSO conditions (weak, moderate and strong) beginning with an strong El Niño/La Niña cycles between 1997 and 1999, followed by weak El Niño between 2002–2004, and finally a moderate El Niño during 2006–2007. Additionally, during the 2002–2004 the California Current System (CCS), remains in the cold phase, a state it has had since the 1999 La Niña phase with the constant permanence of the largest intrusion of subarctic water reported in the last 50 yr characterized as a cold and fresh anomaly in the upper halocline (Huyer, 2003; Goericke, et al., 2005).

In this study, we explored the interannual covariance between SST and chlorophyll *a* (Chl *a*) off Punta Eugenia, an adequate area as a reproductive habitat due to high levels of biological production and its responses to two different large scale processes; the ENSO cycles and the intrusion of subarctic water. Individual and joint empirical orthogonal functions (EOF) analyses were used to extract the principal modes of interannual

Interannual correlations between SST and Chl *a*

H. Herrera-Cervantes et al.

Title Page

Abstract

Introduction

Conclusions

References

Tables

Figures



Back

Close

Full Screen / Esc

Printer-friendly Version

Interactive Discussion



variability and correlations patterns to analyze statistically the temporal and spatial coupled modes of variability between SST and Chl *a* and their response to warming and cooling climate processes. Additionally, we examining the relationship between time series of coastal Chl *a* and wind stress anomalies during 2002–2004 within 50 km of the Northeast Pacific coast (22° N to 45° N).

2 Data and methods

The data used in this analysis are monthly composites of SST and Chl *a* satellite images covering September 1997 through December 2007 for an area from 26–29° N and 113–116° W, centered at Punta Eugenia (see Fig. 1). This data are derived from Advanced Very High Resolution Radiometer (AVHRR-Pathfinder) sensor for SST and sea-viewing wide field-of-view sensor (SeaWiFS) for Chl *a*, available at their respective addresses (<http://podaac.jpl.nasa.gov/> and <http://oceancolor.gsfc.nasa.gov/SeaWiFS>). The initial resolution of 9 km × 9 km for Chl *a* was sampled at a 4 km × 4 km cell size to generate monthly averages with the same spatial resolution for SST, rotating and orienting the images along the coast.

Indices of the intensity of large-scale, wind-induced coastal upwelling (CUI) are generated by the NOAA/NMFS Pacific Fisheries Environmental Laboratory (PFEL) at 15 standard locations along the west coast of North America (Schwing et al., 1996; <http://www.pfeg.noaa.gov/>). We used the CUI centered on 27° N, 116° W as representative of the Punta Eugenia coastal region, filtering out the seasonal cycle by subtracting the corresponding climatological monthly average (CUI interannual anomalies time series). ENSO activity was represented by The Multivariate El Niño Index (MEI), a measure of the variability of the Pacific (Wolter and Timlin, 1993; Behrenfeld et al., 2006). Monthly MEI data were obtained from the Climate Prediction Center of the National Center of Environmental Prediction at the National Oceanic and Atmospheric Administration (NOAA-CPC-NCEP; <http://www.cpc.ncep.noaa.gov>). Finally, the CUI and MEI

Interannual correlations between SST and Chl *a*

H. Herrera-Cervantes et al.

Title Page

Abstract

Introduction

Conclusions

References

Tables

Figures



Back

Close

Full Screen / Esc

Printer-friendly Version

Interactive Discussion



indices were normalized and smoothed using standard deviation and a running mean of three months to reduce small scale and short term variability.

The monthly composite images of SST and Chl *a*, were arranged in matrices $\mathbf{M}(x, t)$ for each variable, where x stands for the cells of each image and t stands for each month between September 1997 and December 2007 (NT images). To remove the annual and semiannual signals by subtracting a fitted (least squares) periodic function from each pixel time series, the periodic function was defined as:

$$F(t) = A_0 + A_1 \cos(w_1 t - \varphi_1) + A_2 \cos(w_2 t - \varphi_2), \quad (1)$$

where A_0 is the annual mean, A_1 , w_1 , and φ_1 are the amplitude, frequency, and phase of the annual signal and A_2 , w_2 , and φ_2 are the equivalent of the semi-annual signal. Next, we obtained the matrices of SST and Chl *a* anomalies (interannual variability), subtracting from each time series of each cell, its corresponding fitted periodic function (Eq. 1) as:

$$\mathbf{A}(x, t) = \mathbf{M}(x, t) - \mathbf{F}(x, t) \quad (2)$$

Each matrix was transformed into normalized anomalies $\text{NA}(x, t)$ by dividing $\mathbf{A}(x, t)$ series by its standard deviation (series were re-scaled to make them comparable). The resulting $\text{NA}(x, t)$ matrices of both variables were used in the individual EOF analysis to identify the dominant modes of SST and Chl *a* interannual variability and its evolution over time (principal components). Joint SST and Chl *a* EOF are calculated from the covariance matrix constructed from both variables to highlight how they covary with each other, forcing them to have the same temporal variability (Wilson and Adamec, 2001). To isolate and spatially localize important coupled modes of variability, homogeneous correlation (Bretherton, et al., 1992) are calculated for two subsets of the time series; between September 1997 to December 1999 to the ENSO coupled signal and between January 2002 to December 2003 to the subarctic water intrusion signature. High homogeneous correlations (HGs) indicate the regions that contribute the most to the temporal variability.

Interannual correlations between SST and Chl *a*

H. Herrera-Cervantes et al.

Title Page

Abstract

Introduction

Conclusions

References

Tables

Figures

⏪

⏩

◀

▶

Back

Close

Full Screen / Esc

Printer-friendly Version

Interactive Discussion



Chl *a*, and CUI (space-average SST(x, \tilde{t}) and Chl *a* (x, \tilde{t}) and CUI monthly time series), all dominated by strong a seasonal peak, mainly affecting SST. Peaks of Chl *a* and CUI occurring in phase during the spring (March–Jun). The annual cycle for each of the three parameters reveals significant overlap between them.

Figure 3 shows the percentage of variance explained by the first three modes for the different EOF analyses (the individual EOFs and the joint EOF analysis). In the individual analysis, the first three EOFs for both parameters accounted for 92 % and 68 % of the total variance, respectively. The interannual variability of SST and Chl *a* off Punta Eugenia is clearly defined by the EOF₁, which accounted for 78 % and 45 % of the variance respectively, which were statistically different because their error bars do not overlap with their neighbors (North et al., 1982). The correlations between the principal components of each EOF₁ (SST and Chl *a*) and the MEI and CUI anomalies are presented in Table 1. The correlation between the EOF₁ of SST and MEI were high ($R = 0.68$, $P < 0.01$) and low for Chl *a* ($R = -0.23$, $P < 0.01$), and the correlation between the EOF₁ of SST and CUI was moderate ($R = -0.38$, $P < 0.01$) and low with Chl *a* ($R = 0.25$, $P < 0.01$), suggesting that the interannual correlation of both variables is strongly dominated by SST and forced principally by different ENSO conditions (weak, moderate, and strong).

Figure 4 shows the spatial patterns and principal components for mode 1 of the individual EOF analyses (surface plot of the EOF₁ loadings), which account for 78 % and 45 % of the total variance for SST and Chl *a* (with the sign-reversed) respectively. Both spatial patterns showed strong gradients along the coast and high loadings were observed offshore (deep region). The pattern of high SST variability (Fig. 4a), coincide with the pattern of high Chl *a* variability (Fig. 4b), whereas the low SST and Chl *a* variability is showed near to the coast. Overlaid on the spatial component maps are contours of the homogeneous correlation (Bretherton et al., 1992), which is the correlation between the time series of the data at each point and the amplitude time series of the EOF₁ scores (Fig. 4c). High homogeneous correlations indicate the region that contributes the most to the temporal variability. Only correlation contours above 0.7 are

Interannual correlations between SST and Chl *a*

H. Herrera-Cervantes et al.

[Title Page](#)[Abstract](#)[Introduction](#)[Conclusions](#)[References](#)[Tables](#)[Figures](#)[◀](#)[▶](#)[◀](#)[▶](#)[Back](#)[Close](#)[Full Screen / Esc](#)[Printer-friendly Version](#)[Interactive Discussion](#)

Interannual correlations between SST and Chl *a*

H. Herrera-Cervantes
et al.

Title Page

Abstract

Introduction

Conclusions

References

Tables

Figures

⏪

⏩

◀

▶

Back

Close

Full Screen / Esc

Printer-friendly Version

Interactive Discussion

shown (significant at the 99 % confidence level). The principal components joined to the normalized MEI and CUI anomalies, showed similar trends (regression line) and major correlations with the MEI, except during 2002–2004 when the principal component of Chl *a* (SST) showed highest positives (negative) amplitudes. The CUI anomalies showed low correlations with both principal components (Table 1). This indicates that the SST–Chl *a* interannual variability off Punta Eugenia was forced both ENSO-related events and strongly by the cold and fresh intrusion of subarctic water, present during 2002–2004 (Venrick et al., 2003; Bograd and Lynn, 2003, and Durazo et al., 2005; Goericke, et al., 2005), which masked the presence of the weak El Niño event of this period.

Figure 5 shows the spatial pattern of the first mode of the joint EOF₁ analysis for SST and Chl *a* (Fig. 5a, b), accounting for 80 % of the total variance. The amplitude time series corresponding to the joint EOF₁ is not shown since they are identical to those of individual EOF₁ in Fig. 4c (Table 1). The SST and Chl *a* spatial pattern differ to those of the individual EOF₁ (Fig. 4a, b). The primary difference between the individual and joint spatial modes of the SST and Chl *a* is that the coastal and northern region dominates more in the joint EOF. In the joint mode low variability corresponds to the southern and depth region as a continuous feature. The high SST along the coast coincident with the area where coastal trapped waves generated during El Niño event continued its poleward propagation along the west coast of the peninsula (Durazo and Baumgartner, 2002; Dever and Winant, 2002), while high Chl *a* can be associated with remote forcing of northern origin. The spatial distribution of the SST–Chl *a* correlations (Fig. 5c), present the area where both parameters strongly co-vary. This area is enclosed with the highest joint EOF₁ scores (> 2.0) of the SST (Fig. 5a). High correlations ($|R| > 4$) occur in a band parallel to the coast, region where intense coastal upwelling and complex mesoscale variability are found. A consistent inverse relationship is observed between SST and Chl *a* coastal anomalies; an increasing SST anomalies is coupled to decreasing Chl *a* anomalies (during El Niño events), implying increases in sea level that deepen the nutricline, reduce the supply of nutrients and limits Chl *a*

production. High positive Chl *a* anomalies associated with La Niña conditions, may elevate the nutricline, decreasing SST and increase the effects of coastal upwelling.

Figure 6 shows contours of mean homogeneous correlation (HCs) calculated for three subset of the time series in both SST and Chl *a* respectively overlaid on (a) the spatial correlation pattern and (b) the chlorophyll mode to assess what regions dominate during the El Niño period (September 1997 to December 1998), La Niña period (September 1998 to December 2000) and the intrusion of subarctic water period (January 2002 to December 2003). For both SST and Chl *a*, a narrow area confined along the coast dominates during El Niño and La Niña: (solid and dotted contours in Fig. 6a). The combination of the mean sets of HCs distributions is virtually identical to the spatial correlation and the joint EOF patterns, meaning that the physical-biological coupling in the coastal region shown in the Fig. 5, is driven by both increase and decrease of SST and chlorophyll during ENSO cycles.

In contrast, the region that dominates significantly during the intrusion of subarctic water period for both SST and Chl *a* is showed by the mean HCs of > 0.6 (solid contours in Fig. 6b) are all in the deep zone, they occur in the same region as during the entire time series (Fig. 4) and where the individual EOF does show the high variability mainly in the chlorophyll mode. These results indicate that the individual variability pattern of both parameters were driven more by the intrusion of subarctic water than by ENSO cycles, contributing little to the coupled mode. The three sets of HCs in Fig. 6 delineate the regions that contribute the most to the individual and coupled mode during different remote forcing; the coastal area and deep region.

Figure 7 shows the time series of the MEI index (bars) and CUI anomalies (black curve), both compared with the temporal evolution of SST and Chl *a* coastal anomalies plotted in two Hovmöller diagrams (i.e., time series of coastal pixels plotted as contours) from 26° N (at the bottom of the diagrams) to the north of Bahía Vizcaíno (at the top, the black line at the middle indicates the position of Punta Eugenia on the coast). Monthly CUI anomalies time series are partially impacted by the different ENSO cycles (weak, moderate and strong), in phase but negatively correlated with the MEI. Warm (cold)

Interannual correlations between SST and Chl *a*

H. Herrera-Cervantes
et al.

[Title Page](#)[Abstract](#)[Introduction](#)[Conclusions](#)[References](#)[Tables](#)[Figures](#)[⏪](#)[⏩](#)[◀](#)[▶](#)[Back](#)[Close](#)[Full Screen / Esc](#)[Printer-friendly Version](#)[Interactive Discussion](#)

Interannual correlations between SST and Chl *a*

H. Herrera-Cervantes
et al.

Title Page

Abstract

Introduction

Conclusions

References

Tables

Figures

⏪

⏩

◀

▶

Back

Close

Full Screen / Esc

Printer-friendly Version

Interactive Discussion

ENSO events are indicated by orange (blue) bars and are associated with positive (negative) SST coastal anomalies showed in the middle panel. The lower panel shows the evolution of coastal anomalies of Chl *a*. The maximum SST anomalies ($\sim 3^{\circ}\text{C}$) and Chl *a* ($\sim -2\text{mgm}^{-3}$) occurred during the strong 1997–1998 El Niño event reversing the sign during the 1999–2000 La Niña conditions mainly south of Punta Eugenia ($\sim -2^{\circ}\text{C}$ and $\sim 1.8\text{mgm}^{-3}$, respectively). During the weak 2002–2004 El Niño event, both parameters showed unusual behavior along the coast, mainly north of Punta Eugenia; negative SST anomalies (-2.5°C) and positive Chl *a* (2mgm^{-3}). These conditions could be associated with an unusual and strong intrusion of subarctic water to lower latitudes driven by southern part of the California Current (Bograd and Lynn, 2003; Durazo et al., 2005), causing a reversal in environmental conditions opposite to the ocean Pacific variability shown by the MEI in this period. Finally, during the moderate 2006–2007 El Niño, the SST surface anomalies showed the typical influence of a warm ENSO event along the coast, while the Chl *a*, continued showed positive anomalies.

Figure 8 showed the relationship between the wind stress and Chl *a* anomalies along the Northeast Pacific coast (22°N – 45°N) from January 2002 to December 2003. Latitude-time plots of coastal wind stress anomalies (Fig. 8a) and coastal Chl *a* anomalies (Fig. 8b) showed that although the study area (shaded in green) was affected by oceanographic conditions of tropical origin during 2002, high positives anomalies in Chl *a* anomalies during spring-summer could be associated with remote forcing of northern origin (intrusion of subarctic water). Wind stress anomalies were found to start weak southerly of 35°N in early 2002 but become westerly along the coast from July to September 2002. It should be noted that Chl *a* signal off Punta Eugenia, reach values compared to that showed north of 42°N (off Oregon coast), where de presence of the cold and fresh subarctic water masses in the CCS was first noticed (Kosro, 2003; Free-land et al., 2003; Goericke et al., 2005), continuing its presence along the Northeast Pacific coast without any significant attenuation or obscured by the co-occurring 2002–2003 El Niño (Bograd and Lynn, 2003). During spring and summer 2003, continued to show high positives Chl *a* anomalies off Punta Eugenia, while wind stress anomalies

showed a pronounced decline off study area. High positive anomalies of Chl *a* that stalled off Punta Eugenia presented a pattern that is only compared to that bloom off Northern California (40° N), where the wind pattern and the intense coastal upwelling processes, produce the most important Biological Action Centers (BAC) of the western coast of North America characterized by levels of pigment concentration above the average for the coastal zone (Lluch-Belda et al., 2000).

4 Discussion

In this study, we used EOF analysis over satellite-driven SST and Chl *a* anomaly data off Punta Eugenia, which has allowed us a wide view of the biophysical coupling during several ENSO events and the largest intrusion of subarctic water reported during 2002–2003. In addition, we related each SST and Chl *a* series within ~ 40 km closest to the coast off Punta Eugenia to two independent variables, MEI and CUI and we followed the coastal signal of the Chl *a* related to the intrusion of subarctic water (2002–2003) from 22° N to 45° N. To our knowledge, this is the first time that physical-biological covariability driven by remote forcing (tropical and subarctic origin) off Punta Eugenia has been examined at this level of detail.

The spatial patterns of individual EOF₁ (Fig. 4a and b) showed that the interannual variability of SST and Chl *a* are not homogeneous and have a strong gradient that defines one area with contours of HCs values > |0.6| offshore indicate the region that contribute the most of the temporal variability different to that showed by Espinosa-Carreón et al. (2004) when examined the interannual variability of SST and Chl *a* off Baja California during 1997–2002, suggest that the large intrusion of subarctic water was a dominant factor in this type of pattern. Although both patterns are similar, its principal components are markedly different ($R \approx 0.3$; see Table 1). The time series of both principal components compared with the MEI and CUI anomalies (Fig. 4c) indicate that these were forced by ENSO-related events and mainly, at least during the 2002–2003 by the large intrusion of subarctic water (Durazo et al., 2005). During this

Interannual correlations between SST and Chl *a*

H. Herrera-Cervantes et al.

Title Page

Abstract

Introduction

Conclusions

References

Tables

Figures

◀

▶

◀

▶

Back

Close

Full Screen / Esc

Printer-friendly Version

Interactive Discussion



Interannual correlations between SST and Chl *a*

H. Herrera-Cervantes
et al.

[Title Page](#)[Abstract](#)[Introduction](#)[Conclusions](#)[References](#)[Tables](#)[Figures](#)[⏪](#)[⏩](#)[◀](#)[▶](#)[Back](#)[Close](#)[Full Screen / Esc](#)[Printer-friendly Version](#)[Interactive Discussion](#)

the intrusion of subarctic water period. Both spatial patterns showed similar behavior, different to that showed by Espinosa-Carreón et al. (2004), where the most of the signal of nonseasonal variability for pigment concentration is in a narrow coastal band. Neither of this patterns have very large spatial loadings near to the coast, and the HCs > 0.6 delineate the regions where the temporal trend of the data correspond the best to the principal components for that mode and hence delineate the regions that contribute the most to the mode, in this case the individual variability mode is defined as the subarctic water mode.

In contrast, the first co-variability mode is the ENSO mode; its temporal components (not shown) are identical to those of the individual modes (Fig. 4) and their spatial patterns for SST and Chl *a* (Fig. 5a, b) are virtually identical to those of the spatial distribution of the SST–Chl *a* correlations (Fig. 5c), mainly with the SST having spatial correlation of -0.98 , the joint spatial pattern for Chl *a* differ little by having high loadings more evenly centered northern of Punta Eugenia, including Bahía Vizcaíno. In a similar fashion we overlaid on the spatial correlation pattern the mean HCs calculated for three subsets of the time series of SST and Chl *a* corresponding to the periods El Niño, La Niña and the intrusion of subarctic water (Fig. 6). There are not significant changes between the mean HCs distribution during the El Niño and La Niña time period (solid and dotted contours), the region dominated for both events is a narrow coastal band that coincide to those of the spatial distribution of the high correlations ($|R| > 4$).

The HCs distribution calculated for both SST and Chl *a* during the intrusion of subarctic water delimited a different area. The mean HCs for both variables dominate a broad area centered in the western basin where the depth is ~ 1000 m off the coast (Fig. 6c), region that contribute significantly to the SST and Chl *a* individual mode when analyzed over the entire time series. During the intrusion subarctic water, there are mean HCs of > 0.6 that contribute little to the joint mode and overall correlation pattern. The coastal zone in the joint modes (Fig. 5a, b), unlike the individual mode, contribute significantly to the mode and coincide to those of high HCs during El Niño and La Niña time period,

which reflects the stronger representation of the coastal zone in the ENSO mode and in the interannual covariation of SST and Chl *a*.

The SST and Chl *a* anomaly evolutive diagrams (Fig. 7, middle and lower panels) showed that the signals associated to weak 2002–2004 El Niño was masked in surface by the intrusion of subarctic water. Both, MEI and CUI anomalies do not showed relationship with the intrusion of subarctic water during this period. Only during the 1997–2000 and 2005–2006 periods, positives Chl *a* coastal anomalies are in agreement with positives CUI anomalies. Espinosa-Carreón et al. (2004) suggested that on an interannual timescale, changes in the monthly CUI anomalies do not appear to be the primary source of variability in the oceanic parameters like that SST and Chl *a*, since removing the seasonal component results in low correlation values (see Table 1). The chlorophyll bloom of 2002–2003 was greater than during the strong 1999–2000 La Niña, evidencing that the distribution of biological groups in areas as far south as 28° N are influenced mostly by the intrusion of water of northern origin than by events of both local and equatorial origin (upwelling and ENSO event). Durazo et al., 2005 observed the presence of zooplankton groups (chaetognaths) at depths of 100 m associated with water of tropical origin that accompanies El Niño events, but also zooplankton groups (salps) associated with an intrusion of subarctic water.

Figure 8 clearly shows the evolution of exceptionally high Chl *a* concentrations and wind stress positives signals during the 2002–2003 extended more than 3000 km along the western coast of North America from 22° N to 45° N. Wind stress anomalies developed northern of 35° N and strengthened during spring and summer 2002, could be associated with onshore large scale advection induced by winds in the central Pacific (Chelton and Davis, 1982) and coincide with the bloom of positives Chl *a* anomalies in this coastal area. It is noteworthy that bloom of positives Chl *a* anomalies observed off Punta Eugenia during spring and summer 2002, could be compared to those observed northern of 38° N, both as a result of the strong west wind stress anomalies developed in summer 2002 since 45° N to the tip of the Baja California peninsula. This bloom of

Interannual correlations between SST and Chl *a*

H. Herrera-Cervantes et al.

Title Page

Abstract

Introduction

Conclusions

References

Tables

Figures



Back

Close

Full Screen / Esc

Printer-friendly Version

Interactive Discussion



positives Chl *a* anomalies occurs again during summer 2003 coincident with the peaks of amplitude time series of the Chl *a* EOF₁ scores (Fig. 4c).

Our study supports the notion that changes in Chl *a* concentration could be due to other factors such as decadal variability, changes in grazing pressures on the phytoplankton (Lavaniegos et al., 2006; Wilson and Adamec, 2001) that may cause impact on biological communities located along the coast. Gaxiola et al. (2008), using data obtained during IMECOCAL cruises (2001–2007), observed that, the intrusion of subarctic water represented by an anomalous low salinity condition in the southern sector of the California current appears to be coupled with the 2002–2006 warm phase of the Pacific Decadal Oscillation Index (PDO). Neither the local upwelling (represented by the CUI anomalies) nor the zonal Ekman drift velocity used as a proxy for coastal upwelling (Gaxiola et al., 2008) showed signals associated with the presence of the intrusion of subarctic water. In this case, the positives signals of wind stress developed along the coast, were agreement with the bloom of the Chl *a*.

5 Conclusions

The temporal and spatial resolution of SST and Chl *a* satellite data, allowed for observation both separately and jointly on the two fields of the physical-biological coupling during large scale processes that affected the CC region off Punta Eugenia, dynamic region of eddy variability, intense biological productivity and oceanographic transition highly influenced by equatorward flows (e.g. anomalous intrusion of subarctic water) and by subtropical signatures triggered by poleward flow (e.g. ENSO cycles). The individual SST and Chl *a* interannual variability were forced mainly by an unusual enhanced onshore transport of subarctic water from the offshore CC during the period 2002–2004, defined by Goericke, et al., 2005 as a cold phase of the CCS, a state it has had since the 1999 La Niña phase. High loadings were observed offshore, showing a strong gradient along the coast while the physical-biological coupling, showed by the correlation and the joint EOF₁ patterns, was forcing mainly by interannual variability

Interannual correlations between SST and Chl *a*

H. Herrera-Cervantes et al.

Title Page

Abstract

Introduction

Conclusions

References

Tables

Figures

◀

▶

◀

▶

Back

Close

Full Screen / Esc

Printer-friendly Version

Interactive Discussion



of equatorial origin (ENSO events) tightly observed in the alongshore band of ~ 40 km wide.

Although, ENSO events dominate along the time period, the presence of the intrusion of subarctic water off Punta Eugenia as a principal remote forcing dominate the individual interannual variability of both variables. These individual patterns present a similar area were this event dominated, an offshore region where the mean HCs calculated for the intrusion of subarctic water time period in both parameters, where in agreement with the high EOF₁ loadings. This remote forcing combined with the positives coastal wind stress signals, results in a large-scale chlorophyll bloom that extend along more than 3000 km of the Northeast Pacific coast between Oregon and Baja California (22° N–45° N) showing that Punta Eugenia is one of the most important Biological Action Centers (BAC) of the western coast of North America which levels of pigment concentration are compared with that of high latitudes (Oregon coast).

Unlike the data gathered during oceanographic cruises, the data used in this study came from 4 km \times 4 km quadrants, and may properly represent the very near shore environments. The 2002–2004 El Niño was masked by the presence of subarctic water, reversed biological-physical response in the surface mainly north of Punta Eugenia. This condition resulted in an atypical situation, such as abnormal cooling of sea surface together with significant high pigment concentration occurring during a warm ENSO phase (Hereu et al., 2003). Furthermore, this abnormal situation was not associated with upwelling-favorable winds (Durazo, et al., 2005) since monthly CUI anomalies showed in Fig. 4c and zonal Ekman drift velocity (Gaxiola, et al., 2008) were negatives during this period. This results successfully complements the reveled previously by hydrographic surveys (CaLCOFI and IMECOCAL programs) off Baja California.

Acknowledgements. Ira Fogel of CIBNOR provided editorial improvements. We thank the Pathfinder and SeaWiFS Projects and the NASA Physical Oceanography Distributed Active Archive Center for the production and distribution of AVHRR-SST and SeaWiFS data. This research was funded by SAGARPA-CONACYT grant 163322.

Interannual correlations between SST and Chl *a*

H. Herrera-Cervantes et al.

Title Page

Abstract

Introduction

Conclusions

References

Tables

Figures



Back

Close

Full Screen / Esc

Printer-friendly Version

Interactive Discussion



References

- Behrenfeld, M. J., O'Malley, R. T., Siegel, D. A., McClain, C. R., Sarmiento, J. L., Feldman, G. C., Milligan, A. J., Falkowski, P. G., Letelier, R. M., and Boss, E. S.: Climatic-driven trends in contemporary ocean productivity, *Nature*, 444, 752–755, 2006.
- 5 Boehm, A. B., Lluch-Cota, D. B., Davis, K. A., Winnan, C. D., and Monismith, S. G.: Covariation of coastal water temperature and microbial pollution at interannual to tidal periods, *Geophys. Res. Lett.*, 31, L06309, doi:10.1029/2003GL019122, 2004.
- Bograd, S. J. and Lynn, R. J.: Anomalous subarctic influence in the southern California Current during 2002, *Geophys. Res. Lett.*, 30, 8020, doi:10.1029/2003GL017446, 2003.
- 10 Bretherton, C. S., Smith, C., and Wallace, J. M.: An intercomparison of methods for finding coupled patterns in climate data, *J. Climate*, 5, 541–560, 1992.
- Carreón-Palau, L., Carreon. P., L., Guzman Del, P. S. A., Belmar, J. P., Carrillo, J. L., and Herrera, R. F.: Microhábitat y biota asociada a juveniles de abulón *Haliotis fulgens* y *Haliotis corrugata* en bahía Tortugas, Baja California Sur, México, *Cienc. Mar.*, 29, 325–341, 2003.
- 15 Chavez, F. P., Strutton, P. G., Friederich, G. E., Feely, R. A., Feldman, G. C., Foley, D. G., and McPhaden, M. J.: Biological and chemical response of the equatorial Pacific to the 1997–1998 El Niño, *Science*, 286, 2126–2131, 1999.
- Chelton, D. B. and Davis, R. E.: Monthly mean sea level variability along the west coast of North America, *J. Phys. Oceanogr.*, 12, 757–784, 1982.
- 20 Dever, E. P. and Winant, C. D.: The evolution and depth structure of shelf and slope temperatures and velocities during the 1997–1998 El Niño near Point Conception, California, *Prog. Oceanogr.*, 54, 77–103, 2002.
- Durazo, R. and Baumgartner, T. R.: Evolution of oceanographic condition off Baja California: 1997–1998, *Prog. Oceanogr.*, 54, 7–31, 2002.
- 25 Durazo, R., Gaxiola-Castro, G., Lavaniegos, B., Castro-Valdez, R., Gómez-Valdez, J., and Mascarenhas Jr, A. S.: Oceanographic conditions off the western Baja California coast, 2002–2003: a weak El Niño and subarctic water enhancement, *Cienc. Mar.*, 31, 537–552, 2005.
- Espinosa-Carreón, L., Strub, P. T., Beier, E., Ocampo-Torres, F., and Gaxiola-Castro, G.: Seasonal and interannual variability of satellite-derived chlorophyll pigment surface height, and temperature off Baja California, *J. Geophys. Res.*, 109, C03039, doi:10.1029/2003JC002105, 2004.
- 30

Interannual correlations between SST and Chl *a*

H. Herrera-Cervantes et al.

Title Page

Abstract

Introduction

Conclusions

References

Tables

Figures

⏪

⏩

◀

▶

Back

Close

Full Screen / Esc

Printer-friendly Version

Interactive Discussion



Interannual correlations between SST and Chl *a*

H. Herrera-Cervantes
et al.

Title Page

Abstract

Introduction

Conclusions

References

Tables

Figures

⏪

⏩

◀

▶

Back

Close

Full Screen / Esc

Printer-friendly Version

Interactive Discussion



Freeland, H. J., Gatien, G., Huyer, A., and Smith, R. L.: A cold halocline in the northern California current: an invasion of subarctic water, *Geophys. Res. Lett.*, 30, 1141, doi:10.1029/2002GL016663, 2003.

Gallaudet, T. C. and Simpson, J. J.: An empirical orthogonal function analysis of remotely sensed sea surfaced temperature variability and its relations to interior oceanic processes off Baja California, *Remote Sens. Environ.*, 47, 374–389, 1994.

Gaxiola-Castro, G., Durazo, R., Lavaniegos, B., De-la-Cruz-Orozco, M. E., Millán-Nuñez, E., Soto-Mardones, L., and Cepeda-Morales, J.: Pelagic ecosystem response to interannual variability off Baja California, *Cienc. Mar.*, 34, 263–270, 2008.

Goericke, R., Venrick, E., Mantyla, A., Bograd, S. J., Schwing, F. B., Huyer, A., Smith, R. L., Wheeler, P. A., Hoff, R., Peterson, W. T., Chavez, F., Collins, C., Marinovic, B., Lo, N., Gaxiola-Castro, G., Durazo, R., Hyrenbach, K. D., and Sydeman, W. J.: The state of the California Current, 2004–2005: still cool?, *CalCOFI Rep.*, 46, 32–71, 2005.

Hereu, C. M., Jiménez-Pérez, L. C., and Lavaniegos, B. E.: Effects of the El Niño 1997–1998 and the Rapid Transition to Cool Conditions in the Winter 1998–1999 on the Copepods and Salps of the California Current, 3rd International Zooplankton Production Symp., 20–23 May 2003, Gijón Spain, Program and Abstracts, p. 53, 2003.

Huyer, A.: Preface to special section on enhanced subarctic influence in the California Current, 2002, *Geophys. Res. Lett.*, 30, 8019, doi:10.1029/2003GL017724, 2003.

Jacobs, G. A., Hulbert, H. E., Kindle, J. C., Metzger, E. J., Mitchell, J. L., Teague, W. J., and Wallcraft, A. J.: Decade-scale trans-Pacific propagation and warming effect of an El Niño anomaly, *Nature*, 370, 360–363, 1994.

Kahru, M. and Mitchell, B. G.: Influence of the 1997–98 El Niño on the surface chlorophyll in the California Current, *Geophys. Res. Lett.*, 27, 2937–2940, 2000.

Kosro, P. M.: Enhanced southward flow over the Oregon shelf in 2002: a conduit for subarctic water, *Geophys. Res. Lett.*, 30, 8023, doi:10.1029/2003GL017436, 2003.

Lavaniegos, B. E., Jiménez-Pérez, L. C., and Gaxiola-Castro, G.: Plankton response to El Niño 1997–1998 and La Niña 1999 in the southern region of the California Current, *Prog. Oceanogr.*, 54, 33–58, 2002.

Lavaniegos, B. E. and Jiménez-Pérez, L. C.: Biogeographic inferences of shifting copepod distribution during 1997–1999 El Niño and La Niña in the California Current, *Contributions to the Study of East Pacific Crustaceans*, 4, 113–158, 2006.

Interannual correlations between SST and Chl *a*

H. Herrera-Cervantes
et al.

Title Page

Abstract

Introduction

Conclusions

References

Tables

Figures

◀

▶

◀

▶

Back

Close

Full Screen / Esc

Printer-friendly Version

Interactive Discussion



Lluch-Belda, D., Elorduy-Garay, J., Lluch-Cota, S. E., and Ponce-Díaz, G.: BAC Centros de Actividad Biológica del Pacífico Mexicano, Centro de Investigaciones Biológicas del Noroeste, Centro Interdisciplinario de Ciencias Marinas, Consejo Nacional de Ciencia y Tecnología, La Paz, B.C.S., Mexico, 2000.

5 North, G. R., Bell, T. L., Calahan, R. F., and Moeng, F. J.: Sampling errors in the estimation of empirical orthogonal functions, *Mon. Weather Rev.*, 110, 699–706, 1982.

Muciño-Días, M., Sierra-Rodríguez, O. P., Castro, J. J., Talavera, J. J., Turrubiates, J. R., Caballero, F., and Rivera, J. L.: Estado de las poblaciones de Abulon azul *Haliotis fulgens* y amarillo *H. corrugata* por zona reglamentada en la costa occidental de la península de Baja California, Temporada 2003/2004, Dictamen Técnico, Instituto Nacional de la Pesca, Dirección general de Investigación pesquera en el Pacífico Norte, Mexico, 12 pp., 2004.

10 Parés-Sierra, A., Lopez, M., and Pavía, E.: Oceanografía Física del Océano Pacífico Nororiental, in: Contribuciones a la Oceanografía Física en México, Monograf. Ser. vol. 3, Unión Geofísica Mexicana, Puerto Vallarta, México, 1–24, 1997.

15 SAGARPA: Anuario estadístico de pesca, 2001, Comisión Nacional de Pesca y Acuicultura, México, 2001.

SAGARPA: Anuario estadístico de pesca, 2011, Comisión Nacional de pesca y Acuicultura, México, 2011.

Schwing, F. B. and Mendelssohn, R.: Increased coastal upwelling in the California Current System, *J. Geophys. Res.*, 102, 3421–3438, doi:10.1029/96JC03591, 1996.

20 SEMARNAT: Salitrales de San Ignacio, sal y ballenas en Baja California, Secretaria de Medio Ambiente Recursos Naturales, México, 1997.

Soto-Mardones, L., Parés-Sierra, A., García, J., Durazo, R., and Hormazabal, S.: Analysis of the mesoscale structure in the IMECOCAL region (off Baja California) from hydrographic, ADCP and altimetry data, *Deep-Sea Res. Pt. II*, 51, 785–798, 2004.

25 Storch, H. V. and Zwiers, F. W. (Eds.): *Statistical Analysis in Climate Research*, Cambridge University Press, Cambridge, 1999.

Strub, P. T. and James, C.: Altimeter-derived surface circulation in the large-scale Pacific gyres. Part 2: 1997–1998 El Niño anomalies, *Prog. Oceanogr.*, 53, 185–214, 2002.

30 Vega, A. V.: Reproductive strategies of the spiny lobster *Panulirus interruptus* related to the marine environmental variability off central Baja California, México: management implications, *Fish. Res.*, 65, 123–135, 2003.

**Interannual
correlations between
SST and Chl *a***

H. Herrera-Cervantes
et al.

Title Page

Abstract

Introduction

Conclusions

References

Tables

Figures

⏪

⏩

◀

▶

Back

Close

Full Screen / Esc

Printer-friendly Version

Interactive Discussion



Vega, A., Treviño, E., Gracia, G., Espinoza-Castro, L., and Zuñiga-Pacheco, C.: Evaluación de la langosta roja (*Panulirus interruptus*) en la región centro occidental de la península de Baja California, mediante modelos dinámicos de biomasa: puntos de referencia y recomendaciones de manejo, Informe de Investigación, Instituto nacional de la Pesca, Mexico, 21 pp., 2010.

Venrick, E., Bograd, S., Checkley, D., Cummings, S., Durazo, R., Gaxiola-Castro, G., Hunter, J., Huyer, A., Hyrenbach, K., Lavaniegos, B., Mantyla, E. A., Schwing, F. B., Smith, R. L., Syderman, W. J., and Wheeler, P. A.: The state of the California Current, 2002–2003: tropical and subarctic influences vie for dominance, CalCOFI Report, 44, 28–60, 2003.

Wilson, C. and Adamec, D.: Correlation between chlorophyll and sea surface height in the tropical Pacific during 1997–1999 El Niño Southern Oscillation event, J. Geophys. Res., 106, 31175–31188, 2001.

Wolter, K. and Timlin, M. S.: Monitoring ENSO in COADS with a seasonally adjusted principal component index, Proc. 17th Clim. Dynam. Workshop, Norman, OK, NOAA/NMC/CAC, NSSL, Oklahoma Clim. Survey, CIMMS and School of Meteorology, Univ. Oklahoma, Norman, OK, 52–57, 1993.

Wooster, W. S. and Hollowed, A. B.: Decadal scale variations in the eastern subarctic Pacific, I. Winter ocean conditions, in: Climate Change and Northern Fish Populations, edited by: Beamish, R. J., Canadian Spec. Publ. Fish. Aquatic Sci., 121, 81–85, 1995.

Interannual correlations between SST and Chl *a*

H. Herrera-Cervantes
et al.

Table 1. Correlations between principal components from different SST and chlorophyll *a* EOF1 analysis and MEI and monthly CUI anomalies.

	EOF ₁ SST	EOF ₁ Chl	EOF ₁ Joint SST	EOF ₁ Joint Chl	MEI	CUI
EOF ₁ SST	1.0	0.30	0.98	0.24	0.68	-0.38
EOF ₁ Chl	0.30	1.0	0.26	0.98	-0.23	0.25
EOF ₁ Joint SST	0.98	0.26	1.0	-0.30	0.63	0.20
EOF ₁ Joint Chl	0.24	0.98	-0.30	1.0	-0.10	0.20
MEI	0.68	-0.30	0.63	0.10	0.10	-0.41
CUI	-0.38	0.25	0.20	-0.41	-0.41	1.0

[Title Page](#)
[Abstract](#)
[Introduction](#)
[Conclusions](#)
[References](#)
[Tables](#)
[Figures](#)
[⏪](#)
[⏩](#)
[◀](#)
[▶](#)
[Back](#)
[Close](#)
[Full Screen / Esc](#)
[Printer-friendly Version](#)
[Interactive Discussion](#)


Interannual correlations between SST and Chl *a*

H. Herrera-Cervantes et al.

Title Page

Abstract

Introduction

Conclusions

References

Tables

Figures

◀

▶

◀

▶

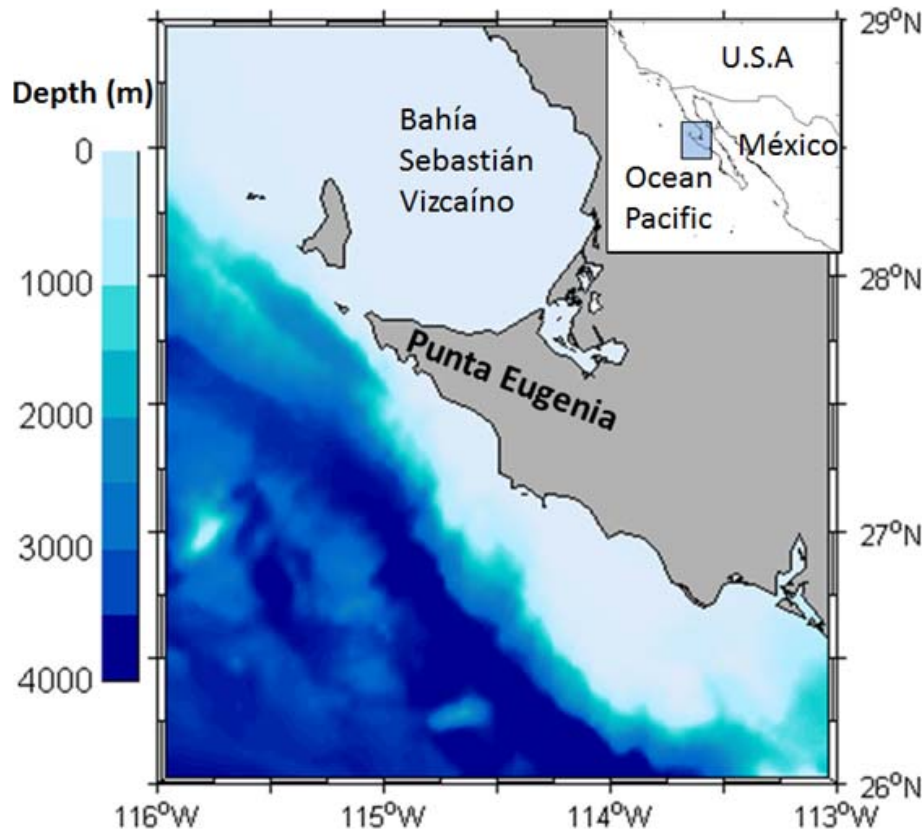
Back

Close

Full Screen / Esc

Printer-friendly Version

Interactive Discussion

**Fig. 1.** Location and bathymetry characteristics of the study area.

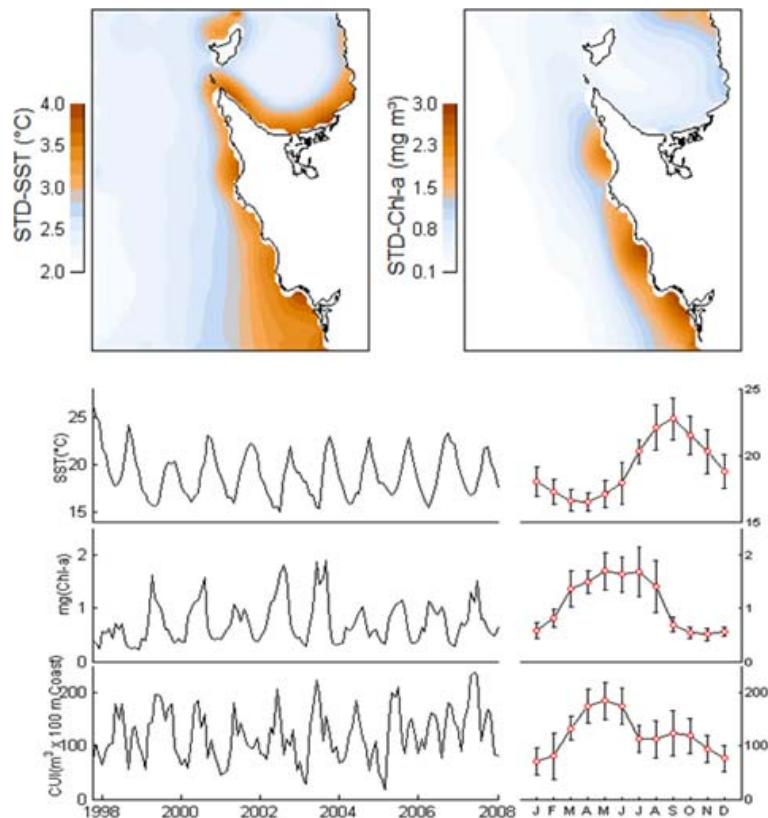


Fig. 2. Standard deviation variability for SST and chlorophyll *a* from September 1997 through December 2007. The time series represent the spatial average of SST and chlorophyll *a* compared with the monthly CUI time series calculated for Punta Eugenia (27° N, 116° W). The curves on the right side correspond to the average seasonal cycle for each variable. Observed averages (red circles) and vertical bars indicate standard deviation.

Interannual correlations between SST and Chl *a*

H. Herrera-Cervantes et al.

Title Page

Abstract

Introduction

Conclusions

References

Tables

Figures

◀

▶

◀

▶

Back

Close

Full Screen / Esc

Printer-friendly Version

Interactive Discussion



Interannual correlations between SST and Chl *a*

H. Herrera-Cervantes et al.

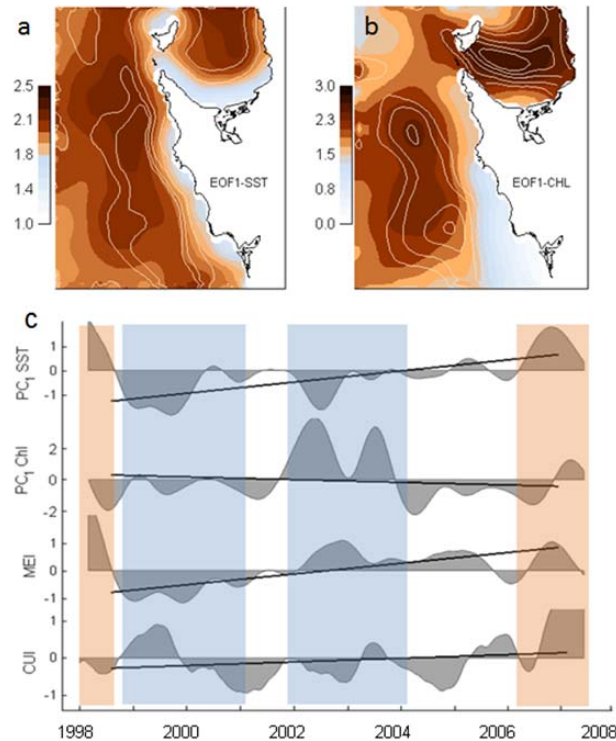


Fig. 4. Spatial patterns for mode 1 of the individual EOF analyses. SST (a), chlorophyll *a* (b), and their corresponding normalized principal components alongside the normalized MEI and monthly CUI anomalies (c). This mode accounts for 78 % and 45 % of the total variance for SST and chlorophyll *a* (with the sign reversed), respectively. Overlaid on the spatial component maps are contours of the homogeneous correlation, the correlation at each point between the time series of the data and the principal components. Trend lines are least-square fits over time in each series. Shaded areas indicate El Niño (red) and La Niña – the intrusion of subarctic water (blue) defined as the cold phase of the California Current System.

Interannual correlations between SST and Chl *a*

H. Herrera-Cervantes
et al.

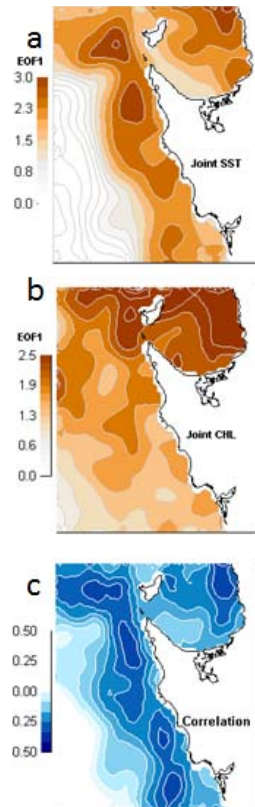
[Title Page](#)[Abstract](#)[Introduction](#)[Conclusions](#)[References](#)[Tables](#)[Figures](#)[◀](#)[▶](#)[◀](#)[▶](#)[Back](#)[Close](#)[Full Screen / Esc](#)[Printer-friendly Version](#)[Interactive Discussion](#)

Fig. 5. Spatial patterns for mode 1 of the joint EOF analyses. SST **(a)**, chlorophyll *a* (with the sign-reversed) **(b)** and **(c)** the correlation map between SST and chlorophyll *a*. The largest positive values of EOF₁ both SST and chlorophyll *a* (> 1.5) and the strongest negative correlation (< -0.3) are alongshore, where SST and chlorophyll *a* are in phase, but negatively correlated.

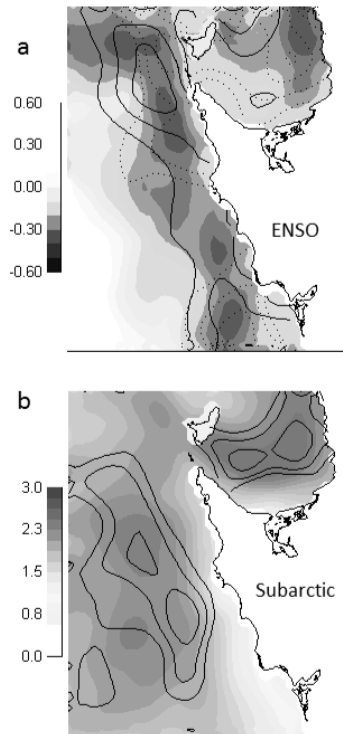


Fig. 6. Contours of mean homogeneous correlation overlaid on **(a)** the correlation map for the El Niño and La Niña period (solid and dotted contours) and **(b)** for mode 1 chlorophyll *a* for the intrusion of subarctic water period (solid contours) using data of both SST and chlorophyll *a*. The El Niño correlation is done using data from September 1997 through December 1998, La Niña correlation is done using data from September 1998 through December 2000 and the subarctic water correlation is done using data from January 2002 through December 2003. The contour interval is 0.1 and the minimum contour shown is 0.6. Absolute correlations above 0.4 are significant at the 99 % confidence level.

Interannual correlations between SST and Chl *a*

H. Herrera-Cervantes et al.

Title Page

Abstract Introduction

Conclusions References

Tables Figures

◀ ▶

◀ ▶

Back Close

Full Screen / Esc

Printer-friendly Version

Interactive Discussion

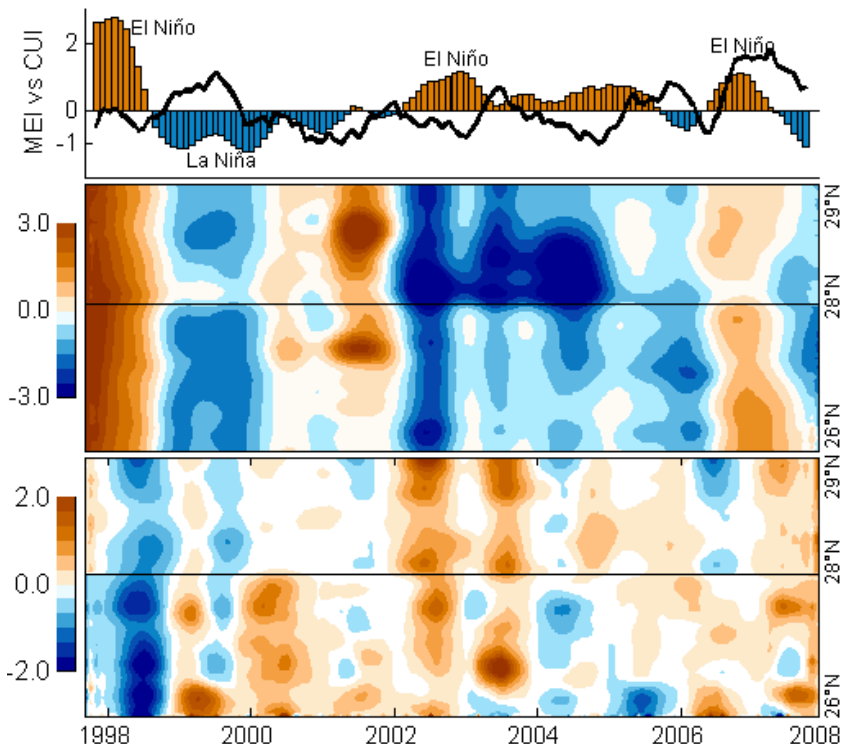


Fig. 7. Temporal evolution of the MEI index (bars, top panel) and monthly CUI anomalies (black curve). El Niño and La Niña episodes are indicate by orange (blue) bars respectively as reports by the Climate Prediction Center of the National Center of Environmental Prediction at the National Oceanic and Atmospheric Administration (CPC-NCEP-NOAA). Hovmöller diagram of monthly averaged coastal SST anomalies (central panel) and chlorophyll *a* anomalies (low panel), from September 1997 to December 2007, covering approximately 300 km of coastline, from 26° N (bottom graph) to 29° N (upper graph). Solid line, indicate the position of Punta Eugenia in the coast (28° N).

Interannual correlations between SST and Chl *a*

H. Herrera-Cervantes et al.

Title Page	
Abstract	Introduction
Conclusions	References
Tables	Figures
◀	▶
◀	▶
Back	Close
Full Screen / Esc	
Printer-friendly Version	
Interactive Discussion	



Interannual correlations between SST and Chl *a*

H. Herrera-Cervantes
et al.

Title Page

Abstract

Introduction

Conclusions

References

Tables

Figures

◀

▶

◀

▶

Back

Close

Full Screen / Esc

Printer-friendly Version

Interactive Discussion

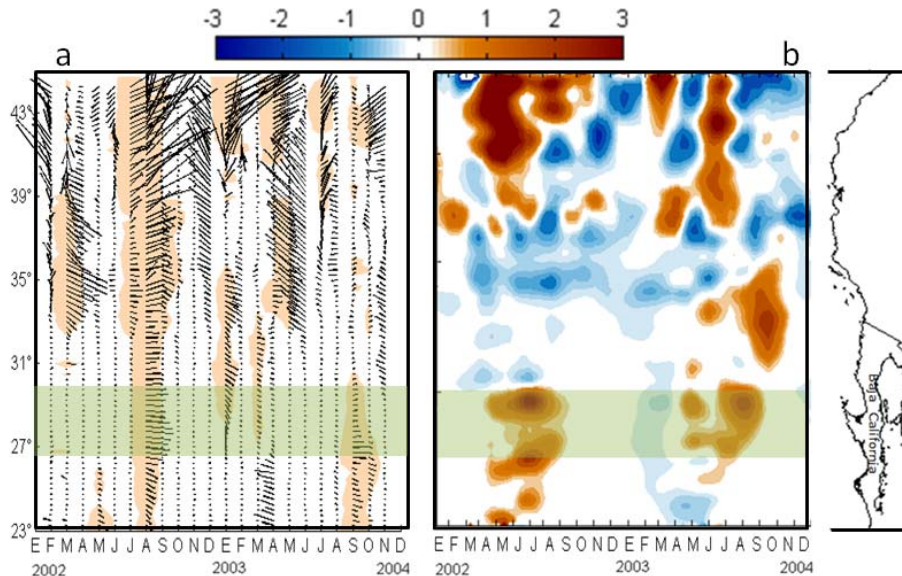


Fig. 8. Hovmöller diagrams of interannual anomalies of **(a)** monthly wind stress ($\text{Nm}^{-2} \times 10^{-2}$), and **(b)** weekly chlorophyll *a* (mg m^3) from January 2002 to December 2003 along the northeast Pacific coast from 22°N to 45°N (values within 50 km of the coast). Both diagrams showed the relationship between wind stress and the presence of the intrusion of subarctic water by summer 2002 off Punta Eugenia coast (green shaded area). The wind data are provided by the Cross-Calibrated Multi-Platform (CCMP) project website at <http://podaac.jpl.nasa.gov/dataset/> and the weekly chlorophyll *a* by the SeaWiFS Project of NASA Goddard Space Flight Center website at <http://oceancolor.gsfc.nasa.gov/>.